Comparative analysis of PM and non-PM design options for small-scale wind generators

Comparative Analysis of PM and Non-PM Design Options for Small-Scale Wind Generators

Nima Arish*, Vahid Teymoori, Lucky Dube, Maarten J. Kamper and Rong-Jie Wang
Department of Electrical and Electronic Engineering, Stellenbosch University, South Africa
*nima.arishh@gmail.com, teymoorivahid@yahoo.com, zebra.lucky@yahoo.com, kamper@sun.ac.za, rwang@sun.ac.za

***Abstract*—For small-scale wind generators to operate efficiently in remote and residential areas, careful consideration must be given to the selection of the generator topology. The purpose of this study is to conduct an in-depth comparison of various design options available for wind generators. These designs include a permanent magnet vernier generator (PMVG), a permanent magnet synchronous generator (PMSG), and a wound-rotor synchronous generator (WRSG). The study thoroughly evaluates various performance aspects, such as cost, efficiency, torque density, power factor, and ripple torque, to help make an informed decision when choosing the most appropriate generator structure for small-scale wind power applications. Evaluation of the designs is validated by comparing two-dimensional finite element results. The findings of this study provide valuable guidance in choosing a generator that is both high-performing and cost-effective for small-scale wind power generation.**

***Index Terms*—Permanent magnet, synchronous generator, small-scale wind generator, vernier generator, wound-rotor**

I. Introduction

In the dynamic realm of sustainable energy solutions, the role of small-scale wind generators has transcended mere functionality to become integral components in a spectrum of applications, ranging from residential installations to commercial enterprises and off-grid environments. The upward trajectory of their adoption underscores the increasing acknowledgment of wind power as a decentralized and environmentally friendly alternative, particularly advantageous in regions endowed with favorable wind conditions. As the prominence of small-scale wind generators continues to ascend, the imperative of selecting the most fitting generator structure becomes an intricate task, with considerations extending beyond mere functionality to encompass critical aspects such as cost efficiency and spatial constraints [1]. PMSG is popular in small-scale wind power systems due to their higher efficiency, compact size, and lightweight design [2]. However, their superior performance comes at a higher cost due to the incorporation of expensive permanent magnets (PM). In contrast, the WRSG is emerging as a popular alternative in wind power systems due to its cost-effectiveness and reliability [3]. However, their cost-effectiveness comes with certain drawbacks. These generators face challenges such as larger physical footprints and utilizing significant amounts of copper in their rotor windings, hence their poor efficiency. Introducing a novel perspective to the domain of PM generators, PMVG emerges as a compelling alternative. By strategically employing a reduced quantity of PMs, the PMVG strikes a delicate balance, offering a cost-effective solution without compromising on essential performance attributes [5], [7]–[12]. This research aims to make a significant contribution to the evolving landscape of small-scale wind power. All the electromagnetic parameters of WRSG, PMSG, and PMVG are comprehensively compared using the Finite Element Method (FEM) to determine the most suitable generator for small-scale wind turbine applications in terms of cost, weight, efficiency, losses, power factor, and torque ripple

The rest of the paper is structured as follows: Section II describes the wind turbine system, Section III field-circuit design approach, Section IV outlines machine topology selection, and Section V electromagnetic comparison, and the conclusions are provided in Section VI.

This work was financially supported by the Department of Electrical and Electronic Engineering, Stellenbosch University in South Africa.

II. Wind turbine System

Fig. 1 shows a proposed small-scale wind energy system utilizing either the PMVG, PMSG, or WRSG generator. The wind turbine with fixed-pitch blades directly connects to the shaft of the chosen generator. The generator converts the wind turbine's mechanical power into AC power, which is synchronously rectified to DC power using a three-phase converter. In the WRSG case, the DC link voltage provides the excitation voltage for the field windings, while the remaining power goes to a DC grid or AC inverter. For PMVG and PMSG, the DC power feeds a DC grid or connects to an AC grid converter.

Fig. 2 presents the characteristics of the small-scale wind turbine. It shows that the 4.2 kW rated turbine power at 320 rpm turbine (generator) speed occurs at 12 m/s wind speed. Additionally, the cut-in turbine speed of 100 rpm at 3 m/s wind speed is shown.

III. Field-Circuit Design Approach

The equations for the PM and non-PM generator options are very similar. We will only discuss the non-PM WRSG equations in detail in this paper. The PM generator equations are simply derived assuming a fixed value for the field current and no field circuit losses. The analysis uses the positive generator model, meaning positive quantities are obtained when electrically positive currents flow out of the generator and mechanically positive torque is anticlockwise.

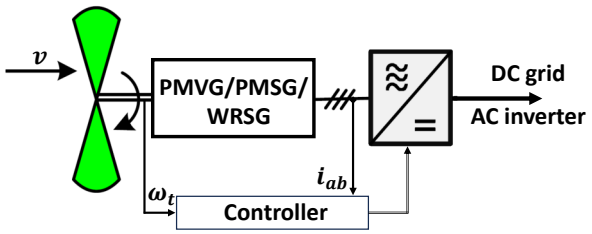

Fig. 1: Schematic diagram of the PMVG- or PMSG- or WRSG-based wind energy system.

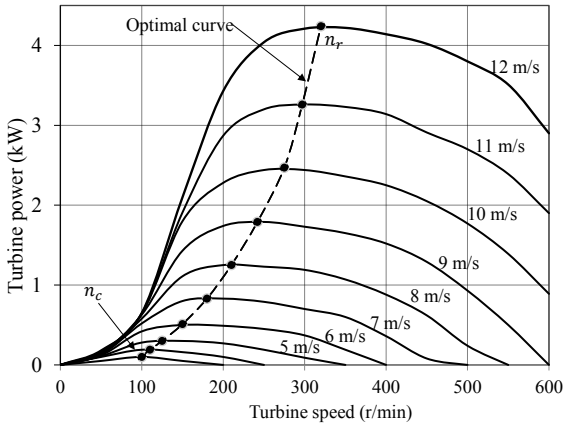

Fig. 2: Turbine power versus turbine speed, with wind speed a parameter.

In the simulation, the finite element analysis software calculates the abc flux linkages as output variables based on the abc current input variables. The dq output flux linkages and dq input currents are determined using the Park or dq transformation. The performance of the WRSG is then determined based on the dq flux linkages and voltages. The dq flux linkages are calculated according to [13]:

$$\lambda_d = \lambda_f - L_d I_d, \tag{1}$$

$$\lambda_q = -L_q I_q, \tag{2}$$

where I_d and I_q are the steady state dq-axis stator currents. L_d and L_q are the dq-axis self-inductances. λ_f is the field inductance and is fixed for the PM generator and $\lambda_f = L_{df} I_f$ for the non-PM WRSG, where L_{df} is the coupling inductance representing the magnetic coupling with the field circuit and I_f is the field current. The dq stator voltages are given by

$$V_d = \omega_e L_q I_q - R_s I_d, \tag{3}$$

$$V_q = \omega_e \lambda_f - \omega_e L_d I_d - R_s I_q, \tag{4}$$

where ω_e is the electrical angular frequency and R_s is the phase-winding resistance. The torque is expressed as

$$\tau_{em} = \frac{3}{2} p(\lambda_d I_q - \lambda_q I_d), \tag{5}$$

where p is the number of pole pairs of the rotor. The dq-axis stator power is given by

$$P_s = \frac{3}{2}(V_d I_d + V_q I_q), \tag{6}$$

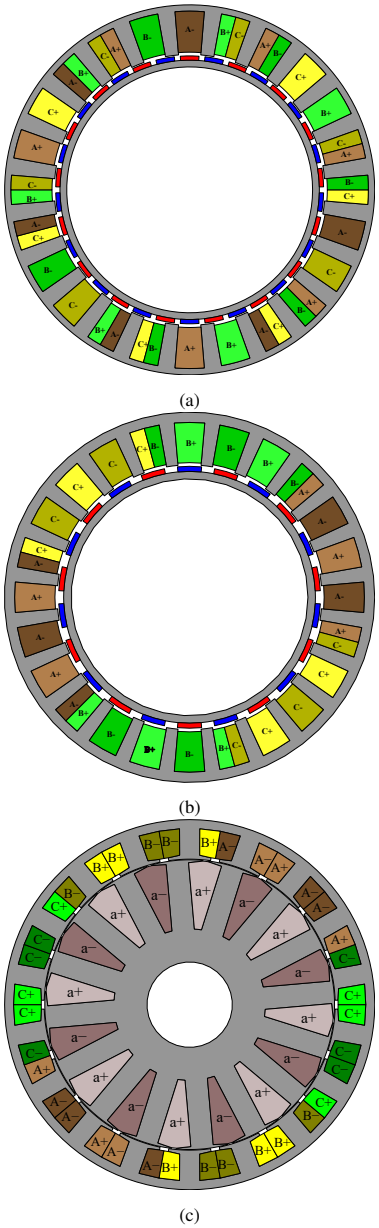

Fig. 3: Cross-section structure of optimum models (a) PMVG 24/34 (b) PMSG 24/22, and (c) WRSG 16/18.

$$S_s = \frac{3}{2}\sqrt{V_d^2 + V_q^2}\sqrt{I_d^2 + I_q^2}. \tag{7}$$

The power factor can then be calculated as

$$P_f = \frac{P_s}{S_s}. \tag{8}$$

The electrical output power, the mechanical input power, and the percentage efficiency are calculated respectively by

$$P_g = P_s - P_{cu(f)}, \tag{9}$$

$$P_t = P_g + P_{cu(f)} + P_{cu(s)} + P_{rot}, \text{and} \tag{10}$$

$$\eta = \frac{P_g}{P_t} \times 100\%, \tag{11}$$

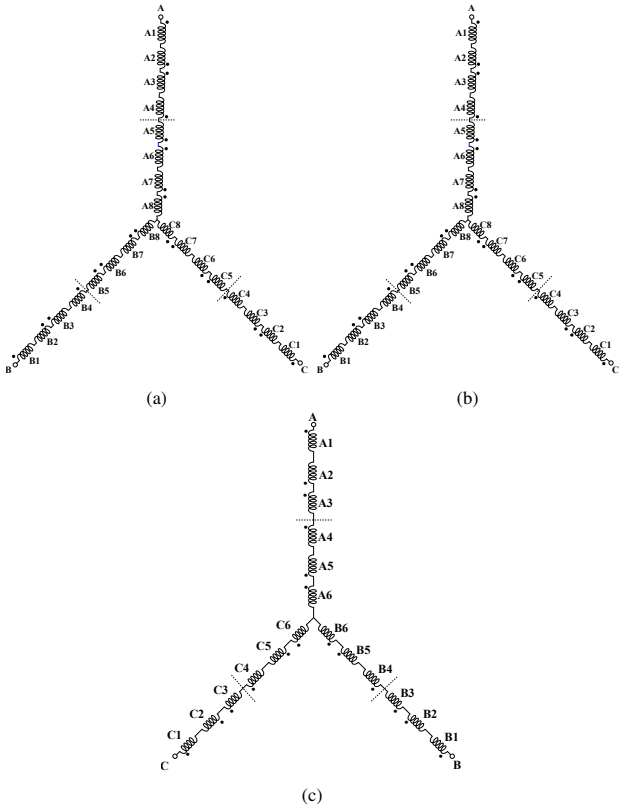

Fig. 4: Winding connection of (a) PMVG 24/34 (b) PMSG 24/22, and (c) WRSG 18/16.

where $P_{cu(f)}$ is the field copper losses (zero for the PM generator), $P_{cu(s)}$ is the stator copper losses and P_{rot} is the total rotational losses.

IV. Machine Topology

As mentioned earlier in this paper, three different structures with different slot/pole combinations—PMSG (24/22), PMVG (24/34), and WRSG (16/18)—are designed and optimized for 4.2 kW small-scale wind turbines. The optimization has been carried out to reduce the mass and size of the generator. The 2D cross-section and winding connections of all optimized models are depicted in Fig. 3 and 4, respectively. Detailed specifications and dimensions of all models are provided in Table I.

TABLE I: Detailed specifications and dimensions of all models.

Parameters	PMVG	PMSG	WRSG
Material	M400-50A	M400-50A	M400-50A
PM	N48H	N48H	-
Slot number	24	24	16
pole number	34	22	18
slot/pole/phase (q)	0.57	0.36	0.37
Fill factor	0.4	0.4	0.45
Outer diameter (mm)	260	260	260
Stack length (mm)	111	120	125
Frequency (Hz)	85	55	42.6
Speed (rpm)	300	300	320
Coil pitch	2	1	1
Winding layer	2	2	2
Winding factor	0.925	0.95	0.945

TABLE II: Electromagnetic performance of all models.

Parameters	PMVG	PMSG	WRSG
Air gap (mm)	1	1	0.45
PM height (mm)	3	3.4	0
PM (Kg)	1.1	1.22	0
Rotor (Kg)	2.1	2.2	17.3
Stator (Kg)	9.3	11.67	10.3
Copper (Kg)	8.1	7	13.5
Total Mass (Kg)	20.6	22.1	41
Material cost ($)	247	258	217
Cost (pu)	1.13	1.18	1
Copper Loss (W)	263	254	707
PM Loss (W)	3.4	5.5	0
Stator Iron Loss (W)	57	62	78
Rotor Iron Loss (W)	9.5	4.5	50
Total Loss (W)	333	327	836
Efficiency (%)	92.3	92.6	80
J (A/mˆ2)	3.6	4	4.8
PF	0.84	0.95	0.8
Ld (mH)	72	54	62.5
Lq (mH)	75.5	62	60
Self Inductance (mH)	95.5	64.5	91.5
Current (A)	6.5	6.6	11.25
Torque (N.m)	131	131	125
Ripple (%)	3.4	2.8	6.5
End Winding Inductance (mH)	4	1	0.6
Stator Leakage Inductance (mH)	23	28.8	12
Torque / Rotor Volume (N.m/m ˆ3)	43	42	30
Torque per Mass (N.m/Kg)	6.35	5.92	2.95

V. Electromagnetic Analysis

All structures were designed and optimized for small-scale, direct-drive, medium-speed wind turbine generators with a frame size of D160. Their electromagnetic performance was compared based on FEM using Ansys Motor-CAD software. Table II provides a comprehensive performance comparison. The PM option designs demonstrate clear weight advantages over the WRSG, with the PMVG excelling particularly in this aspect. Despite the indication of a larger coil pitch, implying an increase in end winding mass, this is effectively counterbalanced by the shorter stack length and reduced PM mass. This combination results in a significantly more compact design, making the PMVG especially well-suited for the application. While PM option designs offer substantial weight advantages due to the higher magnetic flux generated by permanent magnets, the associated cost increase requires careful consideration. Economic viability hinges on a thorough cost-benefit analysis to determine whether the weight reduction justifies the potential rise in generator cost. In this context, WRSGs present a potentially more cost-effective alternative due to the absence of expensive PMs. However, achieving comparable flux levels necessitates increased copper usage in the rotor windings, leading to a thicker and heavier rotor to combat saturation. This solution, while addressing the saturation issue, unfortunately, results in a larger rotor volume and higher copper mass, consequently increasing core and copper losses and impacting overall efficiency. Therefore, the optimal choice between PM and WRSG options depends heavily on the specific application's priorities and constraints. The flux distribution of all models is depicted in Fig. 5. As shown, the possibility of saturation effects in the WRSG is higher than in the others.

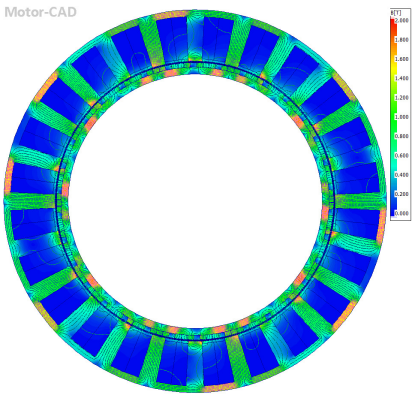

(a)

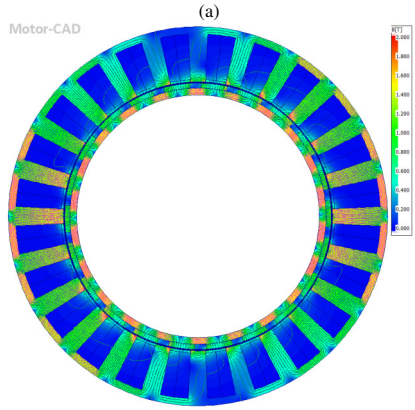

(b)

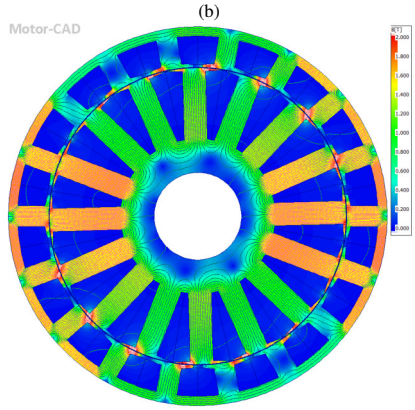

(c)

Fig. 5: Flux distribution of (a) PMVG 24/34 (b) PMSG 24/22, and (c) WRSG 18/16.

A. Airgap flux density

The radial and tangential air-gap flux densities, along with their fast Fourier transform, are depicted in Fig. 6, revealing multiple harmonic components as outlined in Table III. These harmonics are heavily influenced by both the stator and rotor poles. In the PM-based configuration, the amplitudes of the operative harmonic components, denoted as B_t and B_r, are larger than those in the WRSG. In contrast, the amplitudes of the non-working components of B_t and B_r are lower in the PM-based setup compared to the WRSG. This difference could potentially impact core loss and introduce torque ripple, which could affect overall system performance.

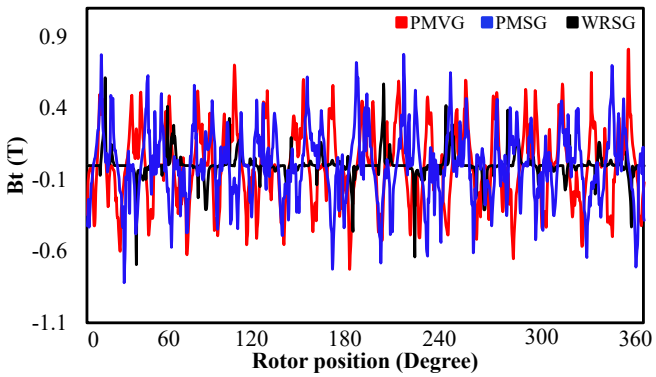

(a)

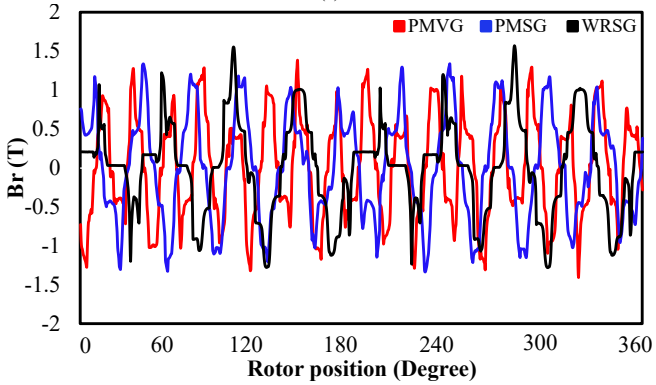

(b)

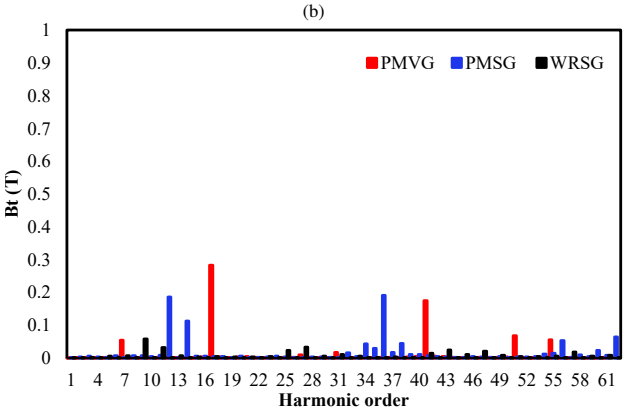

(c)

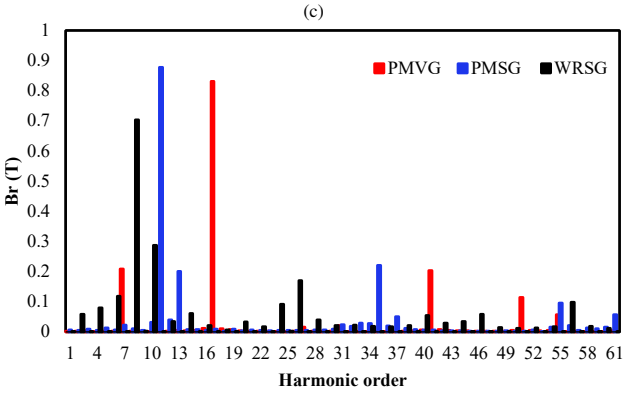

(d)

Fig. 6: Airgap flux density, (a) Bt, (b) Br, (c) magnitude of FFT on Bt, (d) magnitude of FFT on Br.

TABLE III: The radial and tangential airgap flux density per harmonic (v).

PMVG		
v	$B_r(T)$	$B_t(T)$
7	0.2	0.05
17	0.83	0.28
41	0.2	0.17
51	0.2	0.07
55	0.05	0.05
PMSG		
v	$B_r(T)$	$B_t(T)$
11	0.87	0.18
13	0.2	0.1
35	0.22	0.2
37	0.05	0.04
55	0.1	0.05
WRSG		
v	$B_r(T)$	$B_t(T)$
6	0.1	0.01
8	0.7	0.05
10	0.28	0.03
24	0.1	0.02
26	0.17	0.03

B. Loss and EF

In the domain of low-power generators, where efficiency is paramount, a comparative analysis was conducted between PMVG, PMSG, and WRSG. The results showed that PMVGs exhibit nearly identical efficiency to PMSGs despite their higher frequency. Conversely, WRSGs demonstrated significantly lower efficiency due to their reliance on wound rotors for connection. These wound rotors introduce increased resistance, leading to elevated energy dissipation and consequently higher copper and rotor core losses compared to PM-based options. Therefore, the heightened efficiency and lower losses of PM-based options, make them a promising choice for various small-scale wind turbine and energy harvesting systems.

C. PF and cost comparison

In assessing costs, the power factor emerges as a pivotal factor. The WRSG, although potentially boasting lower material costs, introduces a concern regarding its PF. The WRSG tends to exhibit the lowest PF, primarily attributable to its low synchronous inductance [**?**], [14]. It's important to note that the PM-based options present a higher PF compared to the WRSG. The disparity in PF becomes a critical consideration, as a lower PF can significantly impact the cost of associated components like the inverter and converter. While the WRSG may appear to have a cost advantage in terms of materials, the overall system cost may escalate due to the additional expenses tied to compensating for its lower PF. PMSG has the highest PF (0.95) among the three generators, followed by PMVG (0.84) and WRSG (0.8). This means PMSG is the most efficient in terms of power conversion.

D. Torque Analysis

Fig. 7 demonstrates a comparative analysis of torque for all models at a power level of 4.2 kW. As shown, the PM-based options exhibit identical torque values and minimal torque ripple. Conversely, the WRSG displays lower torque due to its higher operating speed, accompanied by a significantly higher torque ripple compared to the PM-based options. The rated torque for the PM-based models is 135 N·m, with corresponding torque ripple values of 3.4% and 2.8% for the PMSG and PMVG, respectively. In contrast, the WRSG exhibits a torque of 125 N·m, with a significantly higher torque ripple of 6.5% due to the higher non-working harmonic, approaching the upper acceptable limit (5%) for this application. The PM-based options demonstrably exhibit lower torque ripple, a crucial factor for small-scale wind turbine applications. This characteristic translates to reduced stress on the drivetrain components, contributing to improved reliability and potentially longer operational life.

E. Thermal Analysis

Thermal analysis is essential for ensuring the safe and efficient operation of electrical machines. During operation, heat generated by internal losses must be removed to prevent overheating and damage to components. Analyzing the temperature distribution within the machine helps determine the need for a cooling system to dissipate excess heat [15]. This paper utilizes the Lumped Parameter Thermal Model (LPTM) implemented in Motor-Cad software to conduct a thermal analysis of all models without a cooling system. This approach allows for a comprehensive evaluation of component temperatures under natural convection conditions. Fig. 8 presents the maximum steady-state temperatures for all models. As shown, the end winding temperatures reach 94°C, 96°C, and 101°C for the PMVG, PMSG and WRSG, respectively. Similarly, the core temperatures reach 93°C, 95°C, and 98°C for the PMVG, PMSG and WRSG, respectively. These results demonstrate the superior thermal performance of the PM-based options compared to the WRSG. This difference may be attributed to the lower overall losses and current density associated with the PM-based designs.

VI. Conclusion

This paper investigated three generator options for 4.2 kW small-scale wind turbine applications: PMVG, PMSG, and WRSG. PM-based options were found to be lighter, more efficient, exhibit lower torque ripple, and have superior thermal performance compared to WRSG, making them a more attractive choice for this application. However, the cost of materials for PM-based options is slightly higher. However,

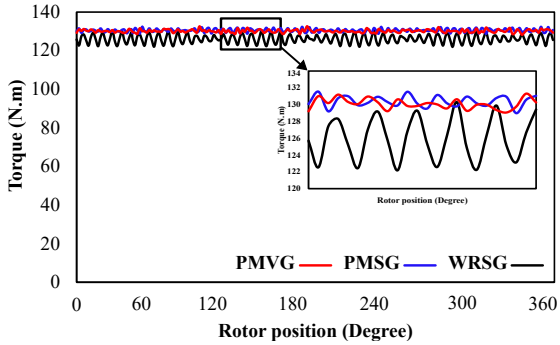

Fig. 7: Torque comparison all models.

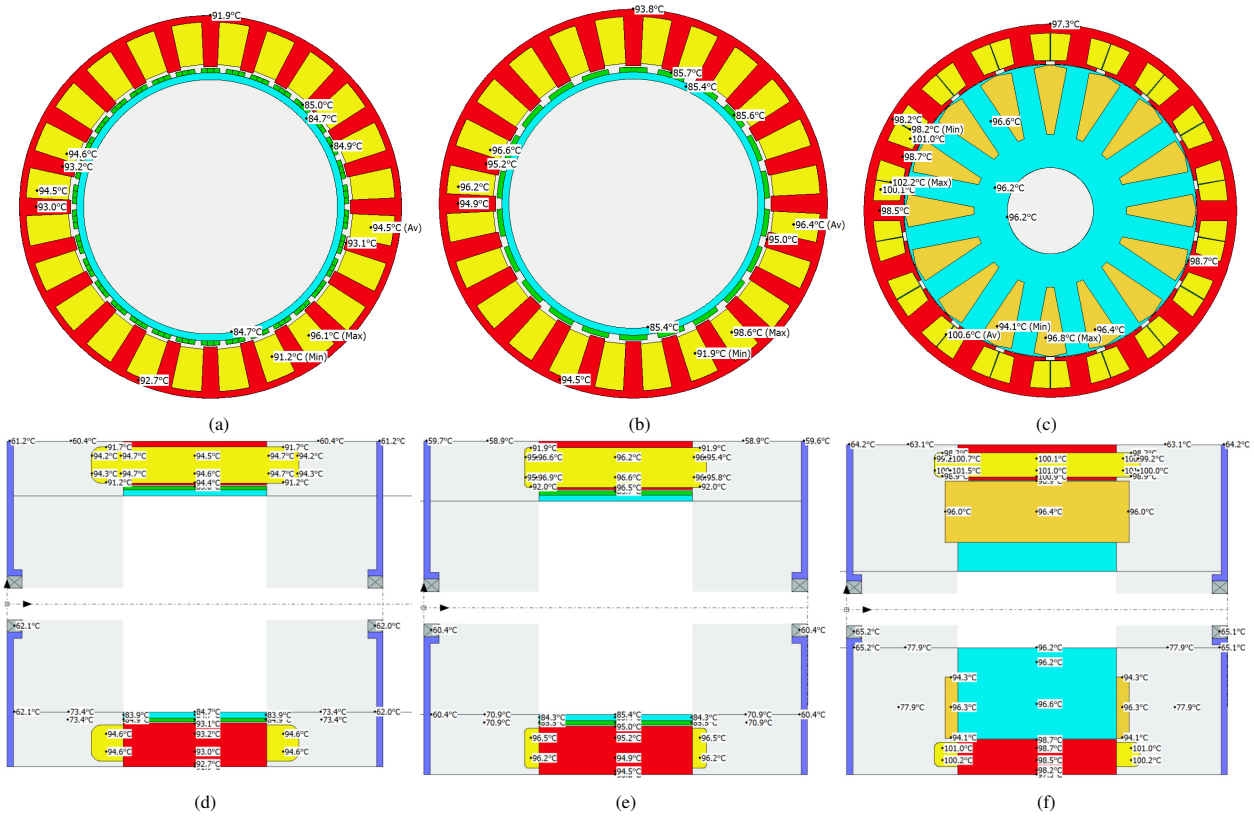

Fig. 8: Thermal comparison without cooling and heat extraction system of (a) radial cross-section of PMVG (b) radial cross-section of PMSG, (c) radial cross-section of WRSG, (d) axial cross-section of PMVG, (e) axial cross-section of PMSG, and (f) axial cross-section of WRSG.

due to the higher PF, especially for PMSG, the total cost of the system can be cheaper due to the lower cost of the converter. Nevertheless, their higher initial cost still needs careful consideration.

REFERENCES

[1] B. Kim, "Design method of a direct-drive permanent magnet Vernier generator for a wind turbine system", IEEE Trans. Ind. Appl., vol. 55, no. 5, pp. 4665-4675, 2019.

[2] G. Friedrich, "Experimental comparison between Wound Rotor and permanent magnet synchronous machine for Integrated Starter Generator applications," 2010 IEEE Energy Conversion Congress and Exposition, Atlanta, GA, USA, 2010, pp. 1731- 1736.

[3] YM. Bash, S. Pekarek, S. Sudhoff, J. Whitmore and M. Frantzen, "A comparison of permanent magnet and wound rotor synchronous machines for portable power generation," 2010 Power and Energy Conference at Illinois (PECI), Urbana, IL, USA, 2010, pp. 1-6.

[4] P. M. Tlali, R.-J. Wang, S. Gerber, C. D. Botha and M. J. Kamper, "Design and Performance Comparison of Vernier and Conventional PM Synchronous Wind Generators," IEEE Transactions on Industry Applications, vol. 56, no. 3, pp. 2570- 2579, May-June 2020.

[5] Desalegn, B.; Gebeyehu, D.; Tamirat, B. Wind energy conversion technologies and engineering approaches to enhancing wind power generation: A review. Heliyon 2022, 8, e11263.

[6] Friedrich, G. Experimental comparison between wound rotor and permanent magnet synchronous machine for integrated starter generator applications. In Proceedings of the 2010 IEEE Energy Conversion Congress and Exposition, Atlanta, GA, USA, 12–16 September 2010; pp. 1731–1736.

[7] N. Arish, M. J. Kamper and R. -J. Wang, "Electromagnetic Analysis of Flux Barrier U-Shaped Permanent Magnet Vernier Motor," 2021 International Aegean Conference on Electrical Machines and Power Electronics (ACEMP) and 2021 International Conference on Optimization of Electrical and Electronic Equipment (OPTIM), Brasov, Romania, 2021, pp. 198-204.

[8] N. Arish, M. J. Kamper and R. -J. Wang, "Performance Comparison of 5-MW Normal and Dual Three-Phase PM Vernier Motors for Ship Propulsion," 2023 International Aegean Conference on Electrical Machines and Power Electronics (ACEMP) and 2023 International Conference on Optimization of Electrical and Electronic Equipment (OPTIM), Istanbul, Turkiye, 2023, pp. 1-8.

[9] N. Arish, M. J. Kamper and R. -J. Wang, "Performance of Large Low-Pole-Ratio Non-Overlap-Winding PM Vernier Motor," 2023 26th International Conference on Electrical Machines and Systems (ICEMS), Zhuhai, China, 2023, pp. 5255-5260.

[10] N. Arish, M. Ardestani and V. Teymoori, "Comparison of Dual Stator Consequent-pole Linear Permanent Magnet Vernier Machine with Toroidal and Concentrated Winding," 2020 11th Power Electronics, Drive Systems, and Technologies Conference (PEDSTC), Tehran, Iran, 2020, pp. 1-5.

[11] N. Arish, V. Teymoori, H. Yaghobi and M. Moradi, "Design of New Linear Vernier Machine with Skew and Halbach Permanent Magnet for Wave Energy Converters," 2019 International Power System Conference (PSC), Tehran, Iran, 2019, pp. 90-94.

[12] N. Arish, H. Yaghobi and V. Teymoori, "Optimization and Comparison of New Linear Permanent Magnet Vernier Machine," 2019 27th Iranian Conference on Electrical Engineering (ICEE), Yazd, Iran, 2019, pp. 657-661.

[13] P. M. Tlali and R.-J. Wang, "PM vernier machine for utility scale wind generator applications: Design and evaluation", Proc. Int. Conf. Elect. Mach., vol. 1, pp. 2637-2643, 2020.

[14] N. N. Siphepho, K. S. Garner and L. Dube, "Effects Of Phase Shifted Three phase Winding On the Performance of A Large Scale Wound Rotor Synchronous Machine," 2023 (ICECCME), Tenerife, Canary Islands, Spain, 2023, pp. 1-5.

[15] A. S. Deaconu, C. Ghiţa, V. Năvrăpescu, A. I. Chirilă, I. D. Deaconu and D. Staton, "Permanent magnet synchronous motor thermal analysis," 6th IET International Conference on Power Electronics, Machines and Drives (PEMD 2012), Bristol, 2012, pp. 1-5.